PNAS
www.pnas.org

Supplementary Information for

Vibration enhanced cell growth induced by surface acoustic waves as in vitro wound-model

Manuel S. Brugger, Kathrin Baumgartner, Sophie. C. F. Mauritz, Stefan C. Gerlach, Florian Röder, Christine Schlosser, Regina Fluhrer, Achim Wixforth and Christoph Westerhausen

Christoph Westerhausen
Email: christoph.westerhausen@gmail.com

This PDF file includes:

Supplementary text
Figures S1 to S5
Legends for Movies S1 to S3
SI References

Other supplementary materials for this manuscript include the following:

Movies S1 to S3

www.pnas.org/cgi/doi/10.1073/pnas.2005203117

Supplementary Information Text

Methods and Materials

SAW-Chip

The key interest of our study lies in the observation that cell growth and cell migration are positively assisted by a SAW-based ultrasonic cell stimulation. The major advantage here is the fact that SAW can be excited on the spot where cells grow and proliferate. For this purpose, SAW are generated on a small piezoelectric chip where micron sized metal electrodes, so-called Interdigital Transducers (IDT) are supplied with an rf signal which then is effectively converted into a well-defined, piezoacoustic surface wave, just like in the above mentioned rf filters in mobile phones. Depending on the desired wave mode, the substrate is chosen to be either $LiNbO_3$ in Y-cut with the crystal axes rotated around the X-axis by 128° (128° rot Y-cut) (LB) or $LiTaO_3$ 40° rot X-Y-cut (LT)(1). The IDT is deposited on top of the substrate by using standard lithography technique. It consists of two multi-finger electrodes (Ti-Au-Ti, d_{Ti} = 5 nm, d_{Au} = 50 nm) and adjusted to the radio frequency (rf)-systems impedance of Z = 50 Ohm, as first described by White and Voltmer(2). The width of the IDT aperture is W = 650 µm and W = 600 µm, respectively. The periodicity of the electrodes in our studies is a = 25 µm and a = 50 µm, respectively which converts to λ_{SAW} = 25 µm and λ_{SAW} = 50 µm. λ_{SAW} and the SAW velocity of the substrate, results in the resonant SAW excitation frequency $f = c/\lambda_{SAW}$. For example, the SAW velocity of LiNbO3, c_{LB} = 3980 m/s, and λ_{SAW} = 25 µm results in f_{res} = 159 MHz. To ensure biocompatibility and to protect the micron sized electrodes, the whole SAW chip except for the contact pads is covered with a 200 nm thick SiO_2 layer. This layer was deposited by thermal evaporation. By feeding a rf-signal of power P_{IN} and frequency f_{res} to the IDT, a spatio temporal, quasi monochromatic and coherently propagating surface deformation, the surface acoustic wave, is generated due to the inverse piezoelectric effect. Dependent on the substrate, cut and transducer design the wave is either a Rayleigh SAW with longitudinal and transversal components for LB or a horizontally polarized love wave for LT(1).

For each experiment and to assess the actual acoustic performance and resonance frequency of the chip, the frequency response is determined beforehand with a network analyzer (NWA) (ZVR, Rhode & Schwarz GmbH & Co. KG., Munich, Germany). The measured frequency-dependent quadripolar reflection coefficient S_{11} is then used to determine the actual resonance frequency and the transconductance of the chip. Typically, for unloaded chips and for the minimal reflection it holds S_{11} < - 18 dB. The rf-power fed into the IDT is measured in mW or dBm, according to the following relation:

$$P_{\mathrm{IN}}(\mathrm{dBm}) = 10\log_{10}\left(\frac{P(\mathrm{W})}{1\ \mathrm{mW}}\right) \quad @\ Z = 50\ Ohm.$$

The simple symmetric IDT design used in this study operates bidirectionally, i.e., it launches SAW in both directions. The acoustic energy P_{SAW} interacting with the cell sample can then be estimated from the minimal reflection value S_{11} and a typical insertion loss of IL ≈ -3 dB. It turns out that P_{SAW} of the propagating wave in our case and for a free substrate surface is P_{SAW} ≈ ¼ P_{IN}. If the thickness of any surface covering material is not negligible as compared to the SAW wavelengths, the SAW is dissipatively attenuated which causes, e.g., the SAW-induced acoustic streaming(3). This out-of-plane-attenuation leads to a 1/e-decay length of the SAW-intensity in propagation-direction which in water turns out to be $l_{\mathrm{op\ X}}^{\mathrm{Calc}} = 12.5 * \lambda_{\mathrm{SAW}} = 331\ \mu\mathrm{m}$ (4). Considering the 1/e-decay length and the aperture width W, the SAW-intensity I_{SAW} acting upon the cells is approximately(4):

$$I_{\mathrm{SAW}} = P_{\mathrm{SAW}}\frac{\left(1-\frac{1}{e}\right)}{W * l_{\mathrm{op\ X}}^{\mathrm{Calc}}} \approx 80\ \frac{\mathrm{mW}}{\mathrm{cm}^2}$$

for P_{IN} = 1 mW and $I_{\mathrm{SAW}} \approx 1\ \frac{\mathrm{W}}{\mathrm{cm}^2}$ for P_{IN} = 13.6 mW. For a more detailed assessment of the SAW-intensities, see our previous work(5). For the rf-signal supply of the IDT, a conventional generator (SML-01, Rhode & Schwarz GmbH & Co. KG., Munich, Germany) and a power amplifier (AMP590033H-T, Becker Nachrichtentechnik GmbH, Asbach, Germany) are used.

Cells and cell culturing

This study comprised two cell lines, 'Madine-Darby Canine Kidney' (MDCK-II) and human osteosarcoma 'sarcoma osteogenic' (SaOs-2). The epithelial cell line MDCK-II (ECACC Cat.No.: 00062107) and the SaOs-2(ECACC Cat.No.: 89050205) were obtained from Sigma Aldrich, Germany. While the MDCK-II cell line provides a perfect model to study epithelia as they have well defined cell junctions, rapid growth rate and a clear apico-basolateral polarity, SaOs-2 cells are suitable to study osteoblastic properties. Additional information on the cell properties can be found elsewhere(6, 7). Both lines were cultured as an adhesive monolayer in the medium recommended by ECACC in NuncTM cell culture flasks (ThermoFisher Scientific, MA, USA) and in a saturated atmosphere with 5 % CO_2 at $T = 37$ °C. The media (SaOs-2: HAMs F12; MDCK-II: MEM Earle´s; Biochrom GmbH, Berlin, Germany) were supplemented with 10 % fetal bovine serum (FPS Superior) and 0.2 % Primocin (InvivoGen, Toulouse, France) for Hams F12 and 1 % Pen/Strep (Biochrom GmbH, Berlin, Germany) for MEM Earle´s. Cell passaging followed the standard trypsinization procedure using 1 ml Trypsin/EDTA (SaOs-2: 0,05 %, MDCK-II: 0,25 %) solution and PBS (w/o Ca^{2+}, w/o Mg^{2+}) (Biochrom GmbH, Berlin, Germany). T-RexTM-293 (HEK293) (Invitrogen, Hennigsdorf, Germany) were cultured in DMEM with Glutamax (Invitrogen, Hennigsdorf, Germany) supplemented with 10% fetal calf serum (Sigma), 1% penicillin/streptomycin (Gibco) and 5µg/ml Blasticidin (Invitrogen, Hennigsdorf, Germany). At least 48h before start of the experiment cells were cultured in antibiotic free medium. Cell density was adjusted to 80.000 cells per 100 µl.

Wound healing assay

If not stated otherwise, for each of the following experiments including cells, a wound healing assay was performed while measuring different cellular parameters. The wound healing assay provides the possibility to monitor the progressive cell migration of two opposing confluent cell layers into a cell-free area. To obtain standardized starting conditions such as confluency, cell density or the width of the cell-free area, a commercially available silicon chamber assay was used. This so called culture insert (CI) (Ibidi ® GmbH, Martinsried, Germany; width 500 µm +/- 50 µm) consists of two chambers with one adhesive side as illustrated in Fig. 1. a-1). Upon confluency, an artificial 'wound' in a confluent cell layer can be created by its removal. After a short delay, cells at the edges of the confluent layers subsequently start to migrate into the empty gap at a constant speed(8).

The experimental setup

The above described SAW-chip was mounted on an in-house made sample holder providing the rf-micro strip lines and connectors to the generator. Contacts between the chip and the board were made by a silver conducting paste (Acheson Silver DAG 1415M, Acheson Industries Inc., MI, USA). To hold the culture nutrient and to house the cells, a polydimethylsiloxane (PDMS) chamber (V = 3 ml) (Sylgard 184 Silicone Elastomer, Dow corning, Germany; m/m ratio 10:1) was placed on top of the SAW-chip. To avoid leakage between chamber and SAW-chip the contact surfaces were coated with a thin layer of highly viscous silicon grease (Baysilicon-Paste, GE Bayer Silicones, Leverkusen, Germany). To maintain sterility of this reusable system, the whole setup was autoclaved at T = 134 °C prior to each experiment and exposed to UV-illumination. Under a microscope, the disposable CI was then carefully placed with its gap oriented parallel to the IDT aperture and about d = 50 µm away from the IDT. Then, 80.000 cells in 100 µl cell suspension were seeded into each of the two chambers of the CI. Upon cell adhesion, the entire chamber was filled with V = 1 ml of nutrient. Subsequently, the cells grew for 24 hours to reach confluency. After the removal of the CI, the cell layers were washed three times with 0.5 ml PBS and refilled with V = 3 ml of fresh nutrient. For the live cell imaging experiments, up to four chips were placed in parallel on the motorized microscope stage (MAC 5000, Ludl Electronic Products Ltd., NY, USA) and connected to a rf-generator. To sustain optimal growth conditions (saturated atmosphere with 5 % CO_2 at T = 37°C) a microscope incubator (ibidi Heating & Gas Incubation System, Munich, Germany) was used. The migration process into the cell-free area was then observed with a microscope (Zeiss Axiovert 200M, Göttingen, Germany) and phase contrast images at multiple positions were taken automatically every five minutes with a 10 x objective.

Measuring intracellular parameters

In order to understand the cellular response and the corresponding biochemical processes behind the SAW-stimulation, different accessible cell parameters are measured. In this study, we determined the production of ROS, the proliferation rate of SAW-stimulated cells and their corresponding internal and external reference. To ensure consistent environmental conditions, the parameters were measured in the framework of a standard wound healing assay. After the removal of the CI, the cells were irradiated by SAW at different power levels while being cultivated in 5 % CO_2 at 37°C (HERAcell® 150 CO_2 Incubator, ThermoFisher Scientific Massachusetts, USA). Depending on the measurand, the measurement protocol was performed during or directly after the treatment as being specified in the following. To detect the cell nucleoli independent from the respective state and size, the DNA binding fluorescent dye Hoechst 33342 (NucBlue® Live ReadyProbes® Reagent, Cat. No.: R37605 - ThermoFisher Scientific, Massachusetts, USA)) was used (ex./em.: ~360/460 nm). Subsequent to the different staining protocols, the samples were analyzed using the previously described microscope at 10 x magnification. Phase contrast and fluorescence images for DAPI (Ex. 350/50 / Em. 460/50 (AHF-F46-000-DAPI, AHF Analysentechnik AG,Tübingen, Germany)) and FITC (Ex. 475/35 / Em. 530/43 (MDF-FITC, Thorlabs Inc, Newton, NJ, USA)) were taken for a large area around the aperture.

ROS: For the detection of ROS, CellROX® Green Reagent (Cat. No.: C10444 - ThermoFisher Scientific, Massachusetts, USA) was used. This fluorogenic probe is cell-permeant and weakly fluorescent while residing in reduced state. Upon oxidation by ROS, and subsequent binding to DNA, the probe exhibits a bright, green and photostable fluorescence (ex./em.: ~485/520 nm). Next to the SAW-stimulated samples, untreated 'low' controls as well as 'high' controls are prepared for each test row. Cells in the 'high' control were treated with 100 µM of menadione (Cat. No.: M2518 – Sigma Aldrich, St. Louis, MO, USA) for 1-hour prior the end of SAW-irradiation. After 24 hours of SAW-irradiation, V = 250 µl of the nutrient supernatant was removed and 40 µM CellROX Green as well as V = 15 µl NucBlue were added and thoroughly mixed. The remaining nutrient was discarded and replaced by the mixture. After 30 minutes of incubation at 37°C and 5% CO_2 the mixture was discarded and the cell layer was washed three times with V = 1 ml PBS and refilled with V = 1 ml fresh nutrient.

Proliferation: To identify proliferating cells in the monolayer the proliferation assay Click-iT™ EdU Cell Proliferation Kit (Cat. No.: C10337 – ThermoFisher Scientific, MA, USA) was used. Here, the modified thymidine analogue EdU is incorporated to freshly synthesized DNA and subsequently labeled with a green fluorescence dye. For detailed information, see the manufacturer's protocol(9). Following the removal of the CI, V = 1 ml of a 20 µM EdU-nutrient solution is added to the culture and the SAW is turned on for 27 hours. The next steps are performed as suggested by the manufacturer.

Data analysis

Wound healing Assays:

The phase contrast images were stitched by a home-made software. The cell-free area was analyzed semi-automatically using the modified ImageJ macro "MRI-Wound healing tool" (http://dev.mri.cnrs.fr/projects/imagej-macros/wiki/Wound_Healing_Tool) and, if necessary corrected manually. In Fig. 1 b) a chronological sequence of a typical experiment at different time points is shown. The cell fronts continuously invade the red-labelled cell-free area over time. Determined by the IDT layout, the width of the sound path is strictly limited to the size of the aperture(10). Therefore, only cells in front and rear of the aperture are directly stimulated by SAW. The cell-free area in this region is called *aperture* in the following. The length of the gap is many times larger than the aperture and its stimulated section. This allows comparison of the SAW-irradiated cells with an internal and natural reference. As shown in the inset of Fig. 1. c) the internal references indicated in green and blue are located next to the wiring. At these positions, the SAW does not interact with the cells. Yet, cells grow under identical conditions (i.e. nutrient supply, temperature, cell density, current cell cycle, viability etc.) as the sample in front of the aperture on the same chip.

In a wound healing assay, a typical parameter is the 'surface area migration rate A_{mig}', which describes the speed of cell migration and growth into the free space. For the evaluation of A_{mig} the cell-free area is determined for every region of interest in Δt = 1.25 h intervals and plotted as function of the elapsed time as shown in Fig. 1. c). The cell-free area *F(t)* was normalized to the cell-free area *F(0)* at the beginning of each experiment. The measured *F(t)* can be approximated by a linear fit. To exclude artefacts in the beginning and at the end of the healing process, only values in the interval $0.8 < F(t) < 0.2$ are taken into account. The slope of the linear fit A_{mig} with the unit area loss in percent per hour. To compare the results and to avoid culture dependent influences, the aperture $A_{mig,\ aperture}$ is divided by the mean of the internal references $A_{mig,\ int.\ ref.}$ shown in Fig. 2 d). This ratio is defined as stimulation efficacy $E := A_{mig,\ aperture}/A_{mig,\ int.\ ref.}$. For each power four separate experiments are performed if not indicated otherwise.
To identify the cell migration over time in one image, grayscale-coded images as shown in Fig. 1 d) are created. One image is the superimposed composition to the complete sequence of one sample. Dependent on the elapsed time, the gray value of the area becomes brighter. We interpret this finding that an early coverage of an area with cells results in a darker color. To maintain a high-quality content of the scientific data, the cell layer in the analyzed region must meet some specific demands like confluency, cell density and viability. As exemplary being shown in Fig. 1 d-3) the right part of the cell layer was not completely confluent as compared to the one in Fig. 1 d-1) - 2). Therefore, only the left part was considered for the internal reference. However, this concerns only a small fraction of all samples.

Fluorescence images:
To evaluate the fluorescence images, the data were analyzed using a self-developed software in MATLAB (MathWorks, Natick, MA, USA). Important MATLAB-specific code commands and parameters are being mentioned in brackets. For evaluation, the recorded 12-bit grayscale images at one position in the DAPI and FITC channel are considered. The phase contrast images were used to verify the cell layer quality qualitatively in the beginning. Next, if necessary, any possible non-uniform illumination in the fluorescence images was rectified using a background image or the mean of all images which had been blurred before. The next steps are dependent on the measurand and are explained briefly:

ROS: The CellROX® Green reagent is a DNA dye and, thus, primarily localizes to the nucleus and mitochondria(11). Detection of the nucleus in the DAPI image is the first step. To accurately distinguish all cells from the background, the images were analyzed using the machine learning algorithm *ilastik: Interactive learning and segmentation toolkit*(12). After removing small objects (*bwareaopen*), the objects were filtered depending on size and subsequently dilated (*imdilate, factor: 2*). Cell clusters are then partitioned by using the watershed-method. This allows to mask the complete area of the nucleus and the one in its close vicinity. The objects' data are then used to calculate the mean gray value of all pixels of one object in the FITC-image. The mean values and their corresponding center coordinates are saved and exported and analyzed depending on the region. The ROS concentration in the 'high' control, however, can vary quite strongly. To only take the maximum concentration for the 'high' control into account, the mean value of the upper five percent of the complete 'high' control sample is evaluated. To avoid errors from the actual condition of the cells, the 'high' control is calculated from the mean of all performed samples. Yet, the related low control is determined separately for each experiment.

Stress level – ROS
Estimating negative effects induced by high SAW-intensities by measuring the intracellular concentration of reactive oxygen species (ROS). SI-Fig. 5 a), a typical image of the intracellular stress of SAW-stimulated cells at a power level of PIN = 64 mW is shown. In Fig. 5 b) – d) a zoom in of the region close to the IDT is visible. The quality of the cell layer and possible morphological changes are verified for each sample using phase contrast imaging (Fig. 5 b)). The position information of the nuclei in Fig. 5 c) is used to determine the cellular stress level in Fig. 5 d). To investigate ROS as a function of the applied power level PIN, selected regions indicated by colored rectangles with Δx = 300 µm and Δy = 650 µm are evaluated in Fig. 5 a). Fig. 5 e) displays the power-dependent ROS concentration in the evaluated areas. At very high SAW-

powers (PIN = 128 mW), some cells start to become ripped off the substrate inter alia caused by the high shear stress induced by the acoustic streaming as shown in Fig. 5 f).

Proliferation: The ratio of the number of proliferated cells and the total number of cells was evaluated. By using two DNA-binding dyes (Hoechst 33342 and EdU binding Alexa Fluor® 488), both probes likely locate in the same region having identical surface areas. This allows us to directly compare the total area of labeled cells in the DAPI and FITC channel. Due to the overlapping excitation and emission spectra of the dyes, a fluorescence resonance energy transfer (FRET) occurs, leading to a slightly darker intensity signal of proliferated cells in the DAPI channel compared to the non-proliferated cells. Here, the machine learning algorithm *ilastik* clearly shows its efficiency by detecting all cell nuclei. The binary images of the DAPI and FITC are then separated in the regions of interest (aperture, internal reference). The median size of the cell nuclei is evaluated for each section by using 'Analyze Particles' in ImageJ. Then, the total amount of white pixels in the DAPI and FITC channel is divided by their corresponding median cell size in order to assess the number of cells in the images. The ratio of cell nuclei in the FITC-channel through the total amount of cells in DAPI-channel is the ratio of proliferating cells in the region. The difference in the proliferation is measured by the statistical change in the number of proliferated cells in the sound path compared to a reference.
The data were statistically analyzed using the Student´s t-test (paired, verified by the Levene-test) using the software Microsoft Office - Excel 2016 (Microsoft, Redmond, WA, USA). Results where $p < 0{,}05$ was obtained are statistically significant.

Results and Discussion

Variation of coverage speed

We analyzed the "wound healing speed" along the device, more precise along the cell free area entitled the artificial wound. For this analysis, we analyzed the recorded area in lines with the width of 1000 px. This results in 7 positions along the device. For these stripes we analyzed the migration velocity of the cell front to determine, the point in time when the migration of the cell front stops. The reciprocal value of this time we define as the gap closing speed. The stripes 2 and 7 here mainly cover the regions that we used as internal reference for the data shown in Fig. 2 and 3. Thus, we normalized the gap closure speed to the mean value of these two stripes. The result (SI-Fig. 2) and the according text from the SI below.

The results show that only the region in front of the aperture shows a significant increased gap closure speed (p<5%). However, the direct neighbors show increased values as well ($p \approx 10\%$ and ($p \approx 36\%$). These might be a consequence of some bystander effect that can not be avoided in such a system. This analysis supports our argumentation in the manuscript.

Estimate the electrical stimulation efficacy

In order to assess the stimulation contribution of the SAWs electrical component, we performed an additional reference measurement. Here, the electrical field is weakened by shortening the lateral component with a 10 nm thick Titanium layer. Ensuring biocompatibility, the Titanium layer is covered with a 200 nm thick SiO_2 layer. The SAW-chip consisted of the material LB with an IDT (λ_{SAW} = 25 µm, W = 650 µm) on top. The experiment is performed using SaOs-2 cells.

Estimate the streaming effect

As cells can be influenced by streaming effects we investigated the cell growth of SaOs-2 cells in stirred media. In this experiment, the IDT is placed aside the artificial gap inducing a streaming by the Leaky-SAW. We used the material LB, a wavelength of λ_{SAW} = 25 µm and applied a rf-power of P_{IN} = 4 mW, where we observed a significant increase in the efficacy E in the previous experiments. The SAW-Chip design and the positioning of the CI is displayed in SI Fig. 4 The cell growth in the stirred media is compared to an external reference with a static media. The surface coverage rate A_{mig} is evaluated along the complete gap for both the sample and the external reference. The

determined efficacy E with $E := A_{mig,\ sample} / A_{mig,\ ext.\ ref}$ is calculated on the basis of three separate test runs.

Stress level – ROS

Estimating negative effects induced by high SAW-intensities by measuring the intracellular concentration of reactive oxygen species (ROS). SI-Fig. 5 a), a typical image of the intracellular stress of SAW-stimulated cells at a power level of PIN = 64 mW is shown. In Fig. 5 b) – d) a zoom in of the region close to the IDT is visible. The quality of the cell layer and possible morphological changes are verified for each sample using phase contrast imaging (Fig. 5 b)). The position information of the nuclei in Fig. 5 c) is used to determine the cellular stress level in Fig. 5 d). To investigate ROS as a function of the applied power level PIN, selected regions indicated by colored rectangles with Δx = 300 µm and Δy = 650 µm are evaluated in Fig. 5 a). Fig. 5 e) displays the power-dependent ROS concentration in the evaluated areas. At very high SAW-powers (PIN = 128 mW), some cells start to become ripped off the substrate inter alia caused by the high shear stress induced by the acoustic streaming as shown in Fig. 5 f).

Fig. S1.

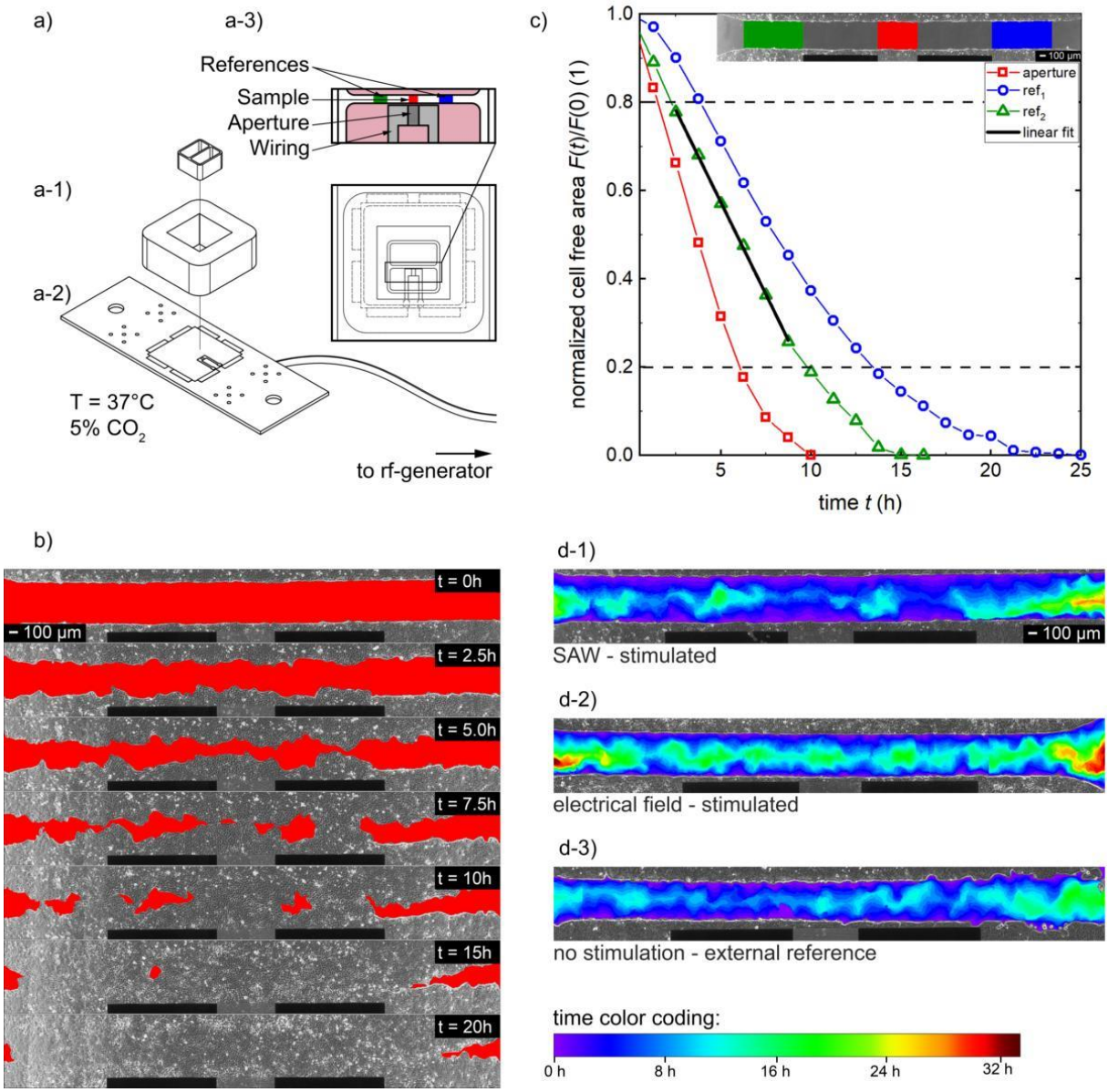

Sketch of the experimental setup and concept of the data analysis. a) Technical drawing of the setup. A culture insert was used to produce a standardized artificial wound in a confluent cell layer (pink) of MDCK-II cells in front of the IDT aperture. b) Time sequenced images of the progressive cell migration of MDCK-II cells into the cell-free area (red). c) Time dependent shrinkage of the normalized cell-free area in the regions of interest (red: stimulated section, green/blue: internal reference). The section between $0.8 < F(t)/F(0) < 0.2$ is approximated by a linear fit. The slope gives the surface area migration rate A_{mig}. d) Superimposed snapshots of the cell fronts of single experiments at different time steps for a time dependent color coded migration progress. d-1)-2) Analyzable samples. d-3) Cell layer quality of the right area does not meet the requirements

Fig. S2.

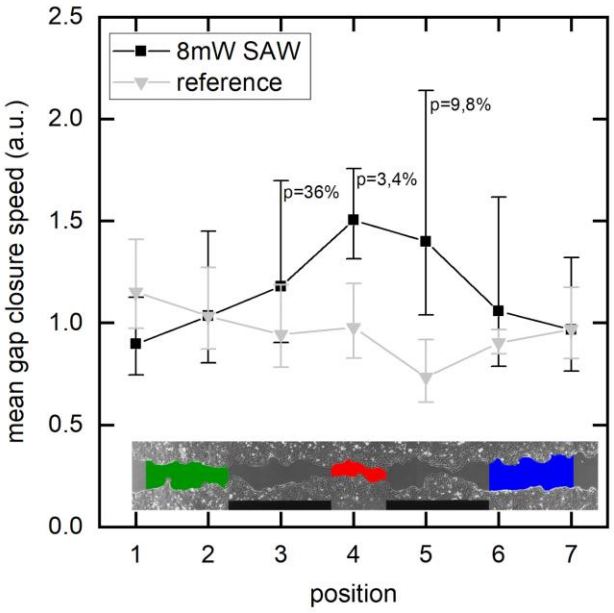

Mean gap closure speed as function of position along the cell free area for MDCKII cells. Position 4 covers the region in front of the aperture, while the internal references are located at about position 2 and 7. Black squares: mean value of n = 4 measurements at a power level of P_{IN}=8 mW. Grey triangles: mean value of n = 4 reference measurements without applied SAW. For the positions 3, 4 and 5 p-values are obtained by a two-sided t-test. Here the results of each position is tested against the results at the internal reference positions 2 and 7.

Fig. S3.

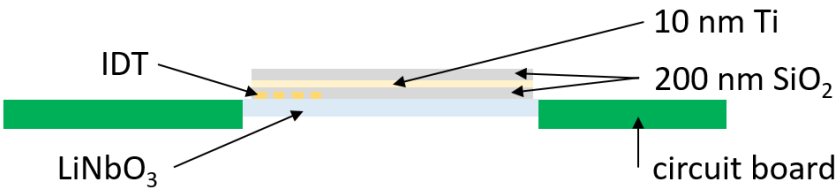

Alternative SAW-chip design to weaken the strength of the electrical field. Using a 10 nm thick Titanium layer on top of the first SiO_2 layer, the lateral electrical field is shortened. SaOs-2 cells were growing on the second SiO_2 layer.

Fig. S4.

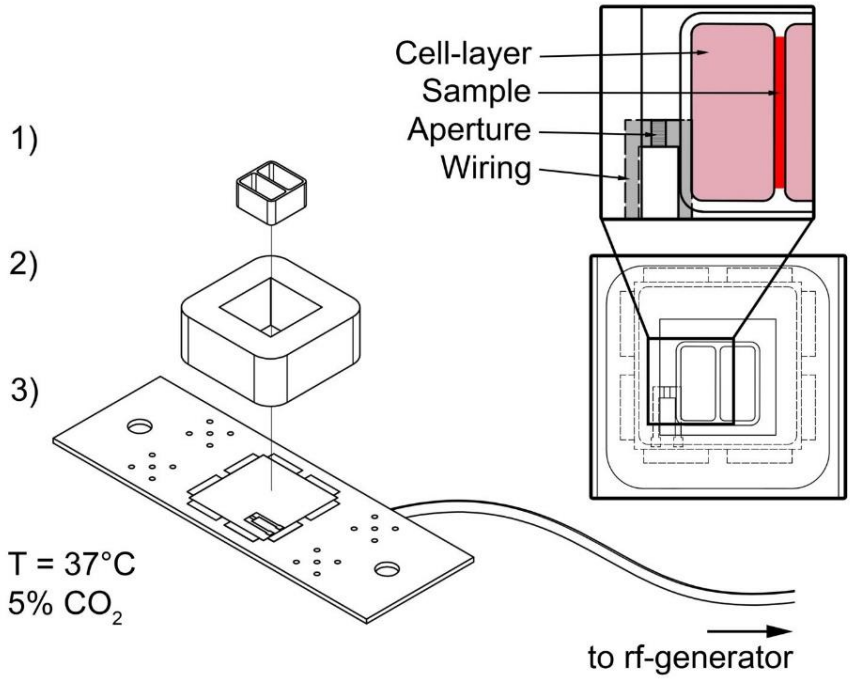

Technical drawing of the experimental setup in exploded- (left) and top-view (right). A culture insert (1)) was used to produce a standardized artificial wound in aside the IDT aperture on a SAW-Chip (3)). The PDMS-chamber (3)) hold the nutrient. The complete gap (red) is used to determine the surface coverage rate A_{mig}.

Fig. S5.

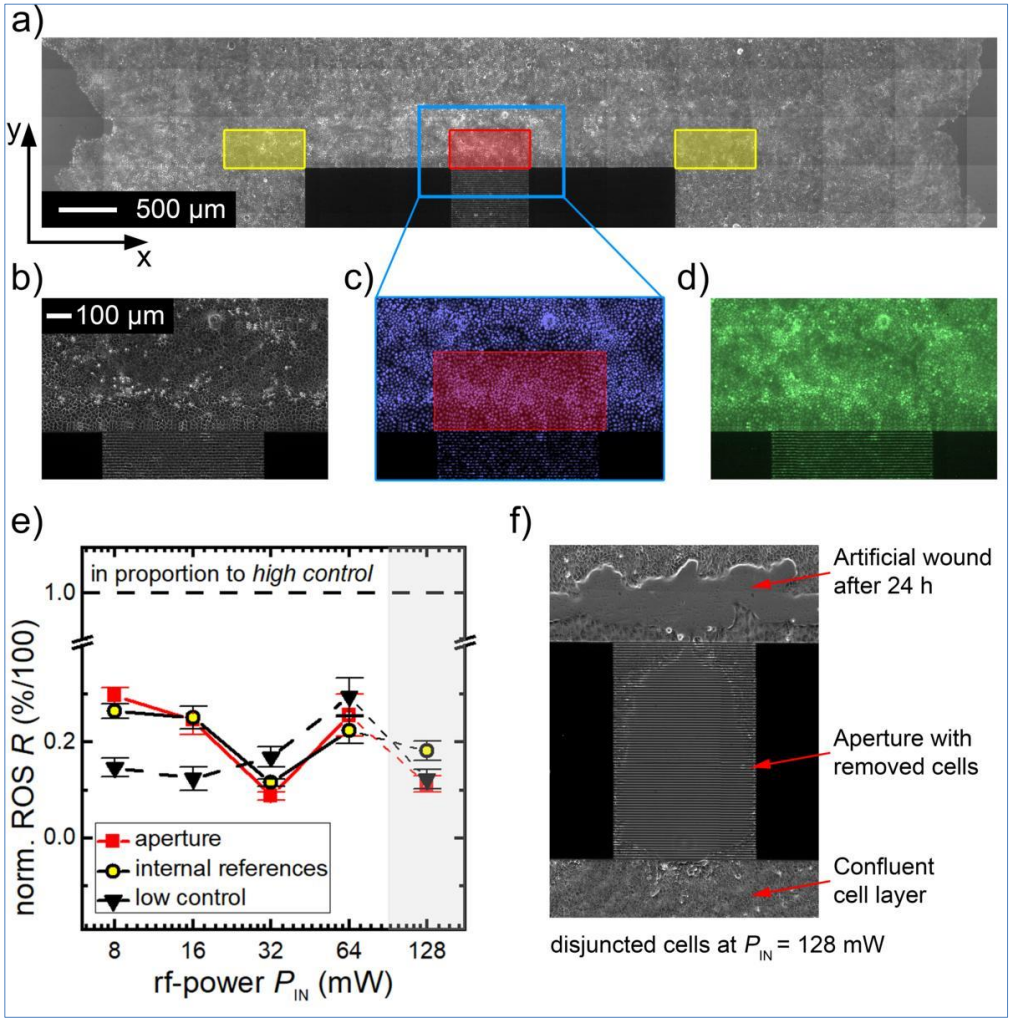

Characterizing the SAW-induced increase of ROS in cells. a) Phase contrast image of the cell layer with evaluated regions marked by colored rectangles (red: aperture, yellow: internal reference). b)-d) Images taken for each measurement: b) phase contrast image, c) cellular nuclei d) ROS in cells. e) Comparison of the ROS concentration relative to the high control. f) Phase contrast image at P_{IN} = 21 dBm.

Movie S1 (separate file). SAW, f=164 MHz, PIN = 16 mW, λSAW = 25 µm, MDCK-II

Movie S2 (separate file). E-field, f=100 MHz, PIN = 16 mW, λSAW = 25 µm, MDCK-II

Movie S3 (separate file). SAW, f=164 MHz, PIN = 16 mW, λSAW = 25 µm, MDCK-II, top: phase contrast image with cell free area labeled in red, bottom: superimposed snapshots of the cell fronts at different time steps with a time dependent color-coded migration progress

SI References

1. D. Morgan, *Surface Acoustic Wave Filters, 2nd Edition*, Second (Academic Press, 2007).
2. R. M. White, F. W. Voltmer, Direct piezoelectric coupling to surface elastic waves. *Appl. Phys. Lett.* **7**, 314–316 (1965).
3. K. Sritharan, C. J. Strobl, M. F. Schneider, A. Wixforth, Z. Guttenberg, Acoustic mixing at low Reynold's numbers. *Appl. Phys. Lett.* **88**, 1–3 (2006).
4. K. Dransfeld, E. Salzman, Excitation, detection, and attenuation of high-frequency elastic surface waves. *Phys. Acoust. Princ. Methods* **VII**, 400 (1970).
5. M. S. Brugger, M. E. M. Stamp, A. Wixforth, C. Westerhausen, Acoustotaxis - in vitro stimulation in a wound healing assay employing surface acoustic waves. *Biomater. Sci.* **4**, 1092–1099 (2016).
6. J. D. Dukes, P. Whitley, A. D. Chalmers, The MDCK variety pack: choosing the right strain. *BMC Cell Biol.* **12**, 43 (2011).
7. S. B. Rodan, *et al.*, Characterization of a Human Osteosarcoma Cell Line (Saos-2) with Osteoblastic Properties. *Cancer Res.* **47**, 4961–4966 (1987).
8. P. K. Maini, D. L. S. McElwain, D. Leavesley, Travelling waves in a wound healing assay. *Appl. Math. Lett.* **17**, 575–580 (2004).
9. T. Scientific, Click-iT EdU Imaging Kits (Manual). *Life Technol. Corp.*, 1–8 (2011).
10. T. Frommelt, "Mischen und Sortieren mit SAW-Fluidik in Simulation und Experiment," Augsburg. (2007).
11. T. Scientific, CellROX® Oxidative Stress Reagents. *Life Technol. Corp.*, 1–6 (2012).
12. C. Sommer, C. Straehle, U. Kothe, F. A. Hamprecht, Ilastik: Interactive learning and segmentation toolkit in *2011 IEEE International Symposium on Biomedical Imaging: From Nano to Macro*, (IEEE, 2011), pp. 230–233.